5/3/02

Installed Transonic 2D Nozzle Nacelle Boattail Drag Study

Michael B. Malone and Charles C. Peavey
Northrop Grumman Military Aircraft Systems Division
Pico Rivera, California 90660

The Transonic Nozzle Boattail Drag Study was initiated in 1995 to develop an understanding of how external nozzle transonic aerodynamics effect airplane performance and how strongly those effects are dependent on nozzle configuration (2D vs. axisymmetric). MDC analyzed the axisymmetric nozzle. Boeing subcontracted Northrop-Grumman to analyze the 2D nozzle. All participants analyzed the AGARD nozzle as a check-out and validation case. Once the codes were checked out and the gridding resolution necessary for modeling the separated flow in this region determined, the analysis moved to the installed wing/body/nacelle/diverter cases.

The boat tail drag validation case was the AGARD B.4 rectangular nozzle. This test case offered both test data and previous CFD analyses for comparison. Results were obtained for test cases B.4.1 (M=0.6) and B.4.2 (M=0.938) and compared very well with the experimental data.

Once the validation was complete a CFD grid was constructed for the full Ref. H configuration (wing/body/nacelle/diverter) using a combination of patched and overlapped (Chimera) grids. This was done to ensure that the grid topologies and density would be adequate for the full model. The use of overlapped grids allowed the same grids from the full configuration model to be used for the wing/body alone cases, thus eliminating the risk of grid differences affecting the determination of the installation effects. Once the full configuration model was run and deemed to be suitable the nacelle/diverter grids were removed and the wing/body analysis performed. Reference H wing/body results were completed for M=0.9 (a=0.0, 2.0, 4.0, 6.0 and 8.0), M=1.1 (a=4.0 and 6.0) and M=2.4 (a=0.0, 2.0, 4.4, 6.0 and 8.0). Comparisons of the M=0.9 and M=2.4 cases were made with available wind tunnel data and overall comparisons were good.

The axi-inlet/2D nozzle nacelle was analyzed isolated. The isolated nacelle data coupled with the wing/body result enabled the interference effects of the installed nacelles to be determined. Isolated nacelle runs were made at M=0.9 and M=1.1 for both the supersonic and transonic nozzle settings. All of the isolated nacelle cases were run at α=0.

Full configuration runs were to be made at Mach numbers of 0.9, 1.1, and 2.4 (the same as the wing/body and isolated nacelles). Both the isolated nacelles and installed nacelles were run with inlet conditions designed to give zero spillage. This was to be done in order to isolate the boattail effects as much as possible. Full configuration runs with the supersonic nozzles were completed for M=0.9 and 1.1 at α=4.0 and 6.0 (4 runs total) and with the transonic nozzles at M=0.9 and 1.1 at α=2.0, 4.0 and 6.0 (6 runs total). Drag breakdowns were completed for the M=0.9 and M=1.1 showing favorable interference drag for both cases.

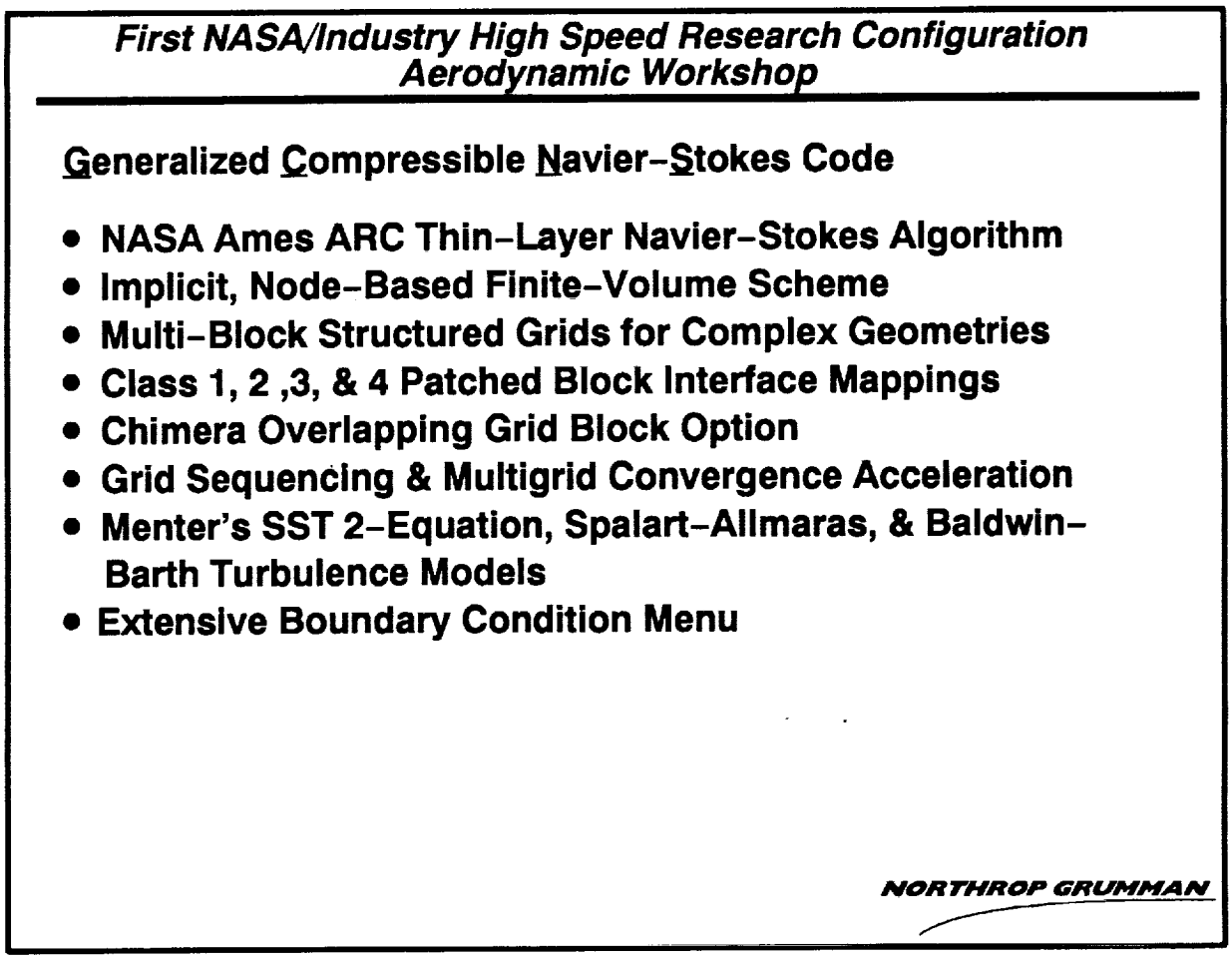

The CFD code used was the GCNSfv developed by Northrop/Grumman. It is based on the ARC3D thin-layer Navier-Stokes algorithm created at NASA Ames . The convergence method is an implicit, node-based finite-volume scheme. Complex geometries are analyzed by using multi-block structured grids. The boundary conditions between blocks can be specified as patched class 1 through 4, where the class 1 is point-to-point macthing, class 2 is incremental point-to-point macthing, class 3 is arbitrary face matching, and class 4 is arbitrary sub-face matching. A Chimera overlapping grid block option is also available. To reduce processing time, grid sequencing and multigrid convergence schemes can be used. GCNS provides three turbulence models to the user: Menter's SST 2-equation model, the Spalart-Allmaras model, and the Baldwin-Barth model. GCNSfv offers a wide variety of boundary conditions including propulsion specific conditions such as characteristic inflow (mass flow ratio and corrected mass flow, inlet bleed) and outflow (nozzle pressure ratio, nozzle temperature ratio) conditions. The code runs at approximately 12 μs/iteration/gridpoint on the Cray C-90 and parallelization allows the code utilize six of the available sixteen processors allowing effective use of the multi-task batch queue.

First NASA/Industry High Speed Research Configuration Aerodynamic Workshop

Transonic Boattail Drag Validation

- **Analyze AGARD 2D Nozzle Test Case B.4**
- **Validate GCNSfv Solution With Test Data**
- **Determine Grid Size and Spacing Requirements to Accurately Model the Flow**

NORTHROP GRUMMAN

The purpose of modeling the AGARD B.4 test case was to validate the Northrop Grumman CFD method (GCNSfv) on a geometry similar to that of the Reference H 2D nozzle nacelles. AGARD test case B.4.2 (M=0.938) is a particularly difficult case with a shock induced separation. The test case was also used to determine the appropriate grid spacings required to accurately model the flow and give some insight on how to build the grids for Reference H configuration.

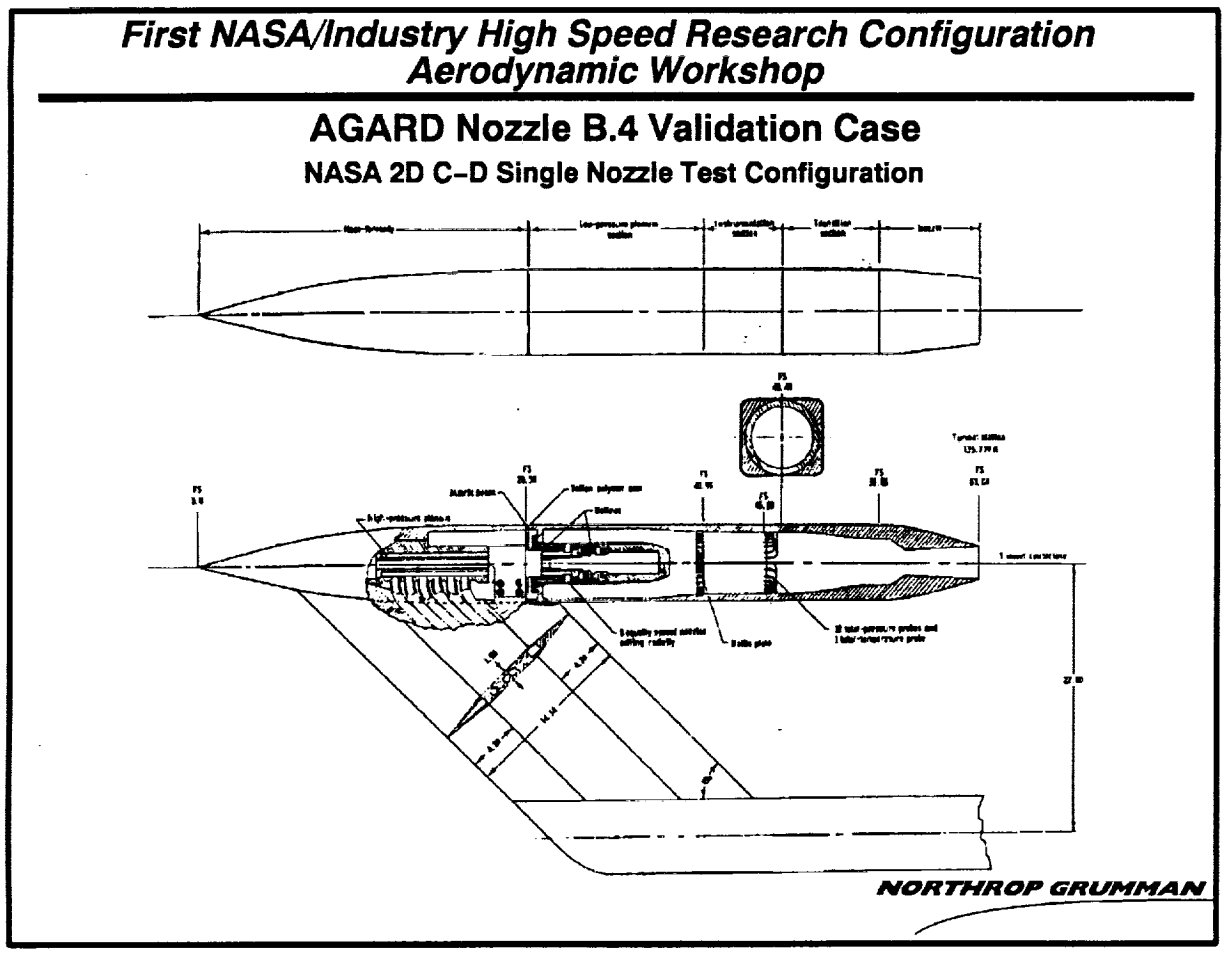

The test configuration for the NASA 2D C–D single nozzle used by the AGARD Working Group #17 "Aerodynamics of 3D Aircraft Afterbodies" for test cases B.4 is shown.

First NASA/Industry High Speed Research Configuration Aerodynamic Workshop

AGARD Nozzle B.4 Validation Case

Computational Grid – Quarter Symmetry

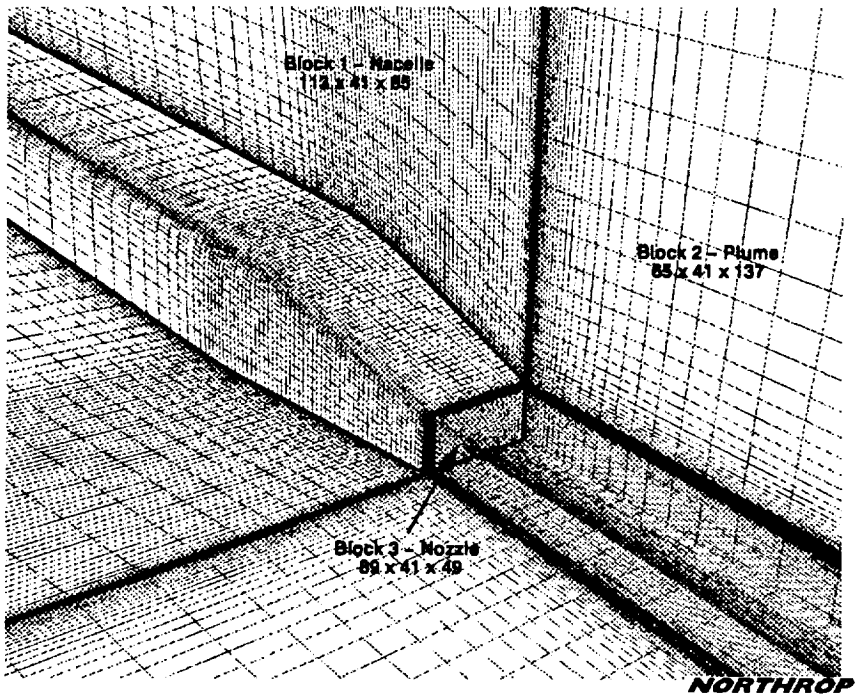

NORTHROP GRUMMAN

The CFD grid for the AGARD nozzle is shown. The outer surface grid of the nacelle was generated from the existing LaRC grid using the identical axial grid distribution while increasing the circumferential grid density. Additionally, the topology of the nozzle and plume blocks were changed and the extent of the grid to the far field was expanded. The test condition of α=–0.02 was approximated as α=0.0 to enable a quarter symmetric model and reduce run time.

Boattail Drag Validation Case

AGARD B.4 Test Case - Drag Convergence History

AGARD Test Case B.4.1

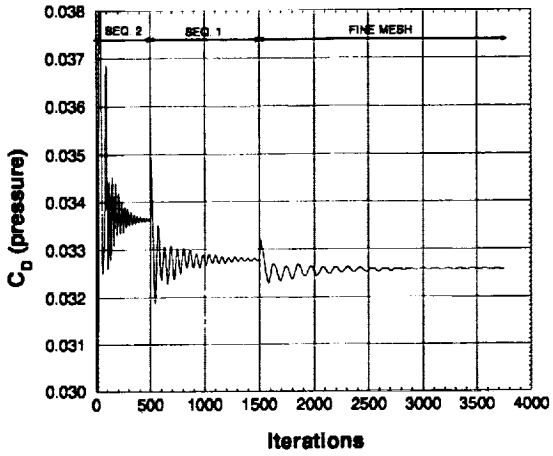

AGARD Test Case B.4.2

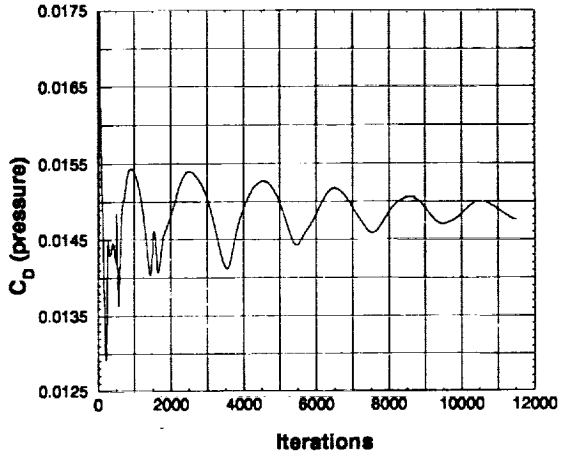

NORTHROP GRUMMAN

Drag convergence histories are plotted for the B.4.1 and B.4.2 test cases. The drag coefficient is only the pressure component, viscous drag calculations are not currently tracked by GCNSfv. The plots illustrate that a lot of iterations are required to converge the transonic (B.4.2, M=0.938) case. The subsonic case (B.4.1, M=0.6) converges very quickly at all sequence levels. Careful monitoring of the solution for the transonic case showed that the shock location and strength set up very quickly, but the separated flow on the nozzle upper surface continued to fluctuate. This is what causes the oscillatory nature seen in the convergence history. Values of y+ were less than 3.0 everywhere on the surface which should be more than adequate for the turbulence model (Menter k–ω SST).

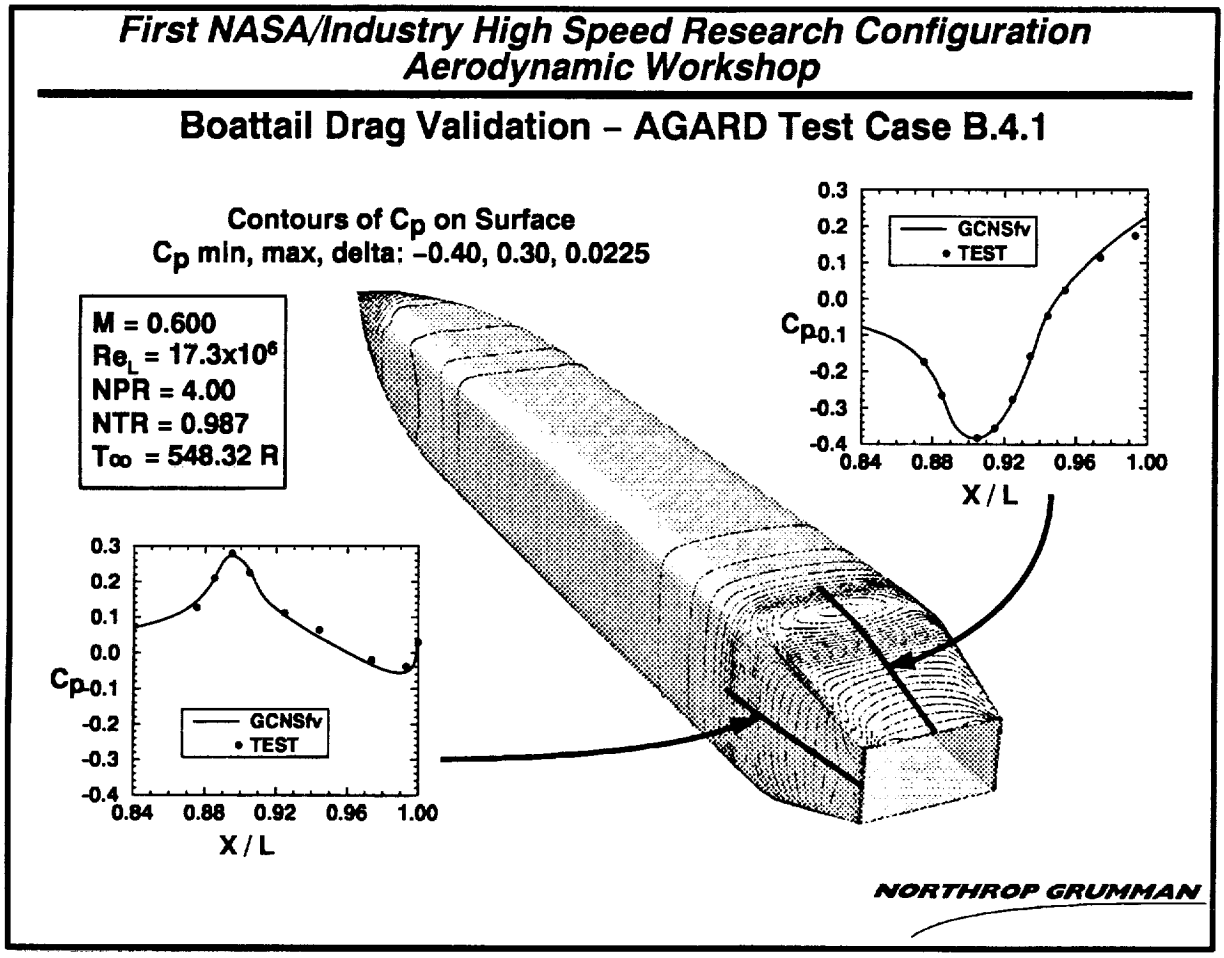

Contours of Cp on the surface are shown for case B.4.1. Flow conditions for test case B.4.1 are M=0.6, Re_L=17.3x10^6, NPR=4.0, nozzle temperature ratio (NTR, T_{tot}/T)=0.987, and free stream static temperature was 548.32 R. Line plots comparing Cp to test data (rows 1 and 5) and their locations are also shown. The solution agrees well with the test data.

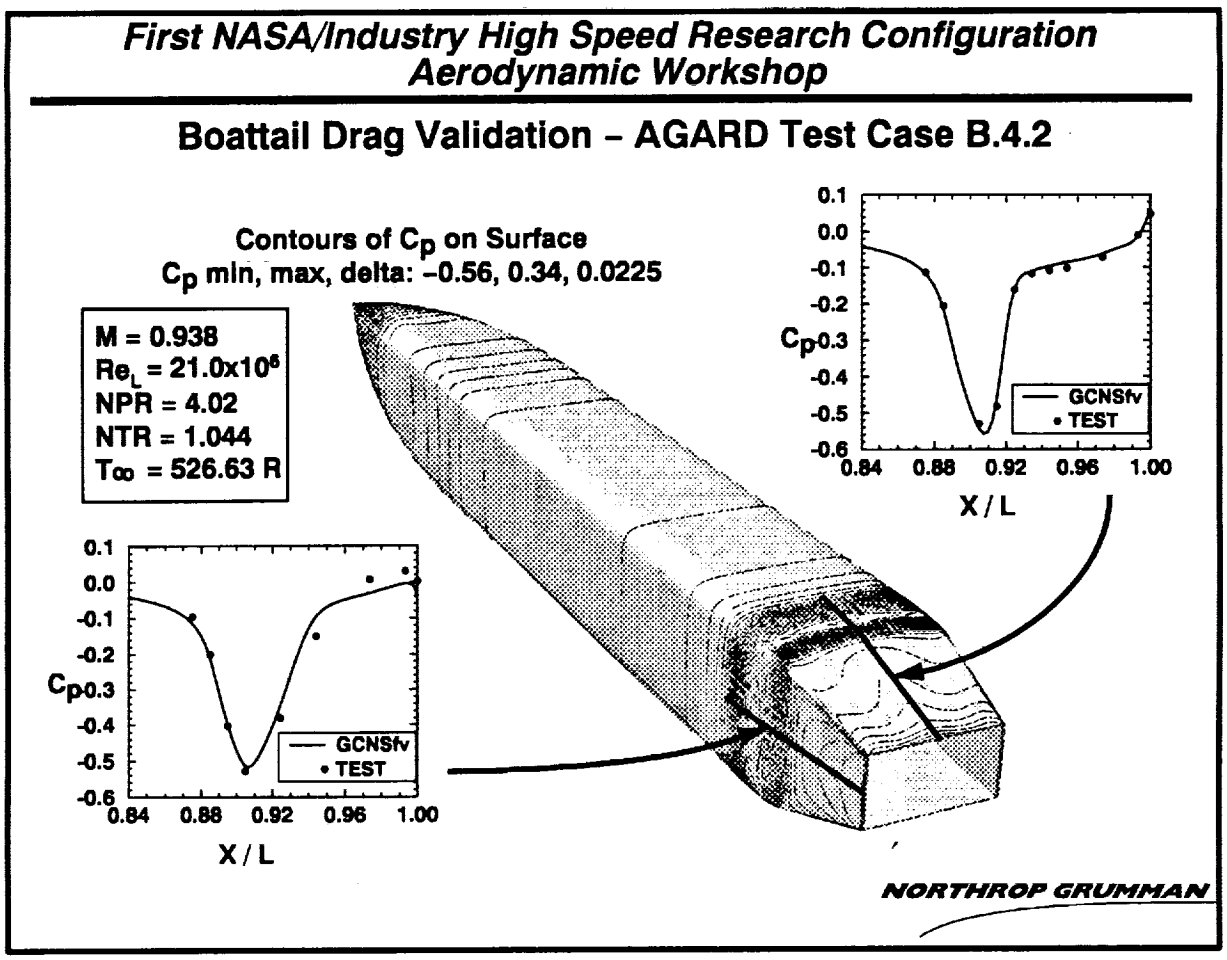

Contours of Cp on the surface are shown for case B.4.2. Flow conditions for test case B.4.2 are M=0.938, Re_L=21.0x10^6, NPR=4.002, NTR=1.044, and free stream static temperature was 526.63 R. Line plots comparing Cp to test data (rows 1 and 5) and their locations are also shown. As shown the solution agrees well with the test data, predicting shock location and strength to give the correct pressure recovery on the upper surface..

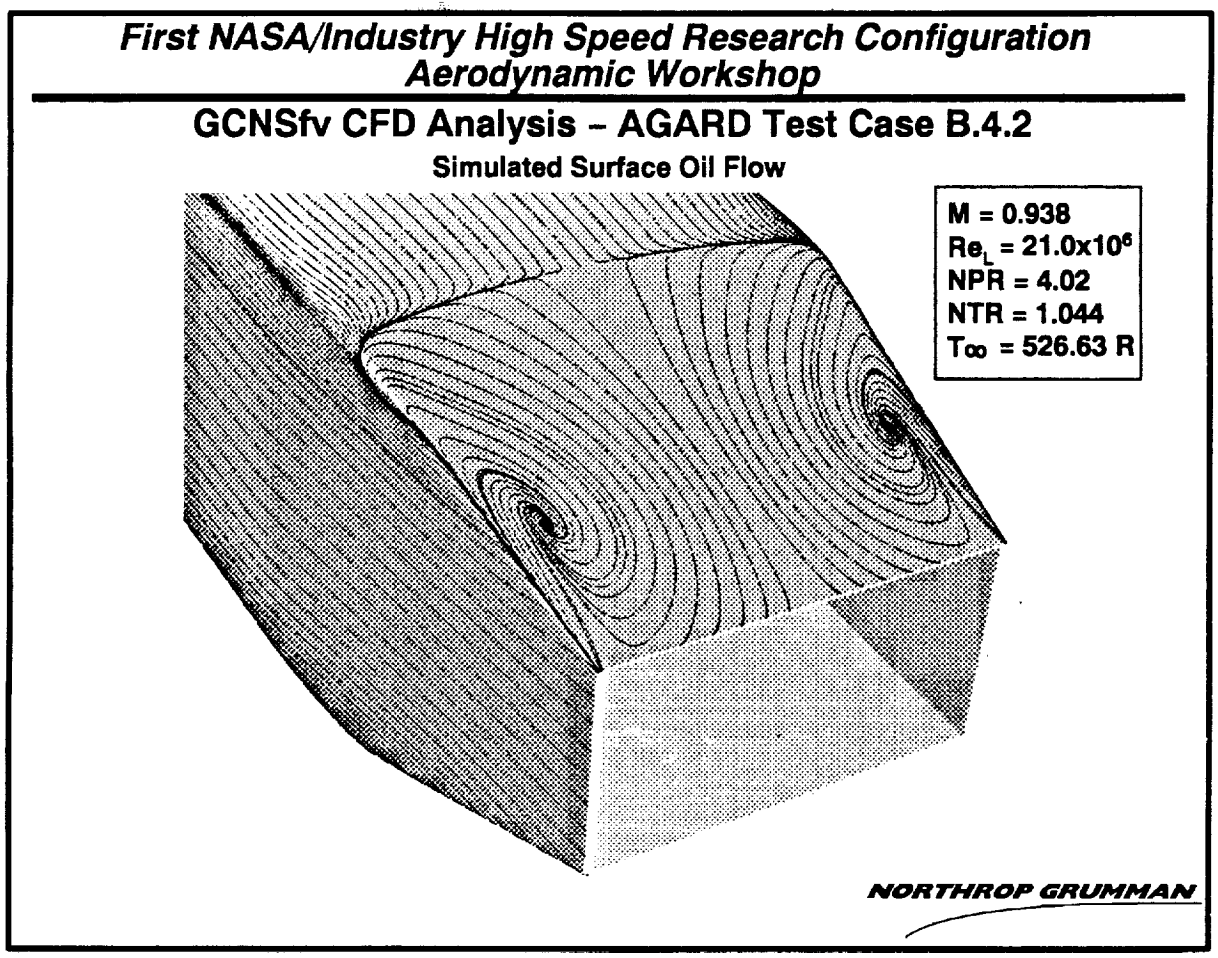

Surface oil flows (streamlines restricted near the surface) are shown for test case B.4.2. The streamlines clearly show the separation line and reverse flow on the rear upper surface.

First NASA/Industry High Speed Research Configuration Aerodynamic Workshop

Wing/Body Validation

- **Model Ref. H Wing/Body (Without Tails) at Re=40 Million**
- **Compare M=0.9 and M=2.4 Runs to Test Data**
- **Use FOMOCO for Force and Moment Integrations**
- **Fuselage Integrated to F.S.=2764.3 to Account for Sting**
- **CFD Data Corrected to Test Reynolds Number Using Flat Plate Skin Friction Data**

NORTHROP GRUMMAN

The wing body runs were made using the grids from the full configuration model. Wind tunnel data was available for M=0.9 and 2.4, although runs were also made at M=1.1 for the interference drag analysis. All of the CFD analysis for this task was run at $Re=40x10^6$. The M=0.9 results were compared to the NTF wind tunnel data at a $Re=30x10^6$ and the M=2.4 results were compared to the ARC 9x7 data at $Re=7x10^6$. The CFD data was corrected to the appropriate Reynolds number using flat plate skin friction corrections. In addition, the fuselage in the CFD analysis was integrated only up to the fuselage station 2764.3 to account for the presence of the sting in this test configuration. The wing/body CFD analysis was used for validation and in the drag buildup calculations. The NASA–Ames integration code, FOMOCO, was used to post–process the (overset grid) solutions and produce the total force and moment coefficients including pressure and viscous contributions.

First NASA/Industry High Speed Research Configuration Aerodynamic Workshop

Wing/Body - Drag Convergence History

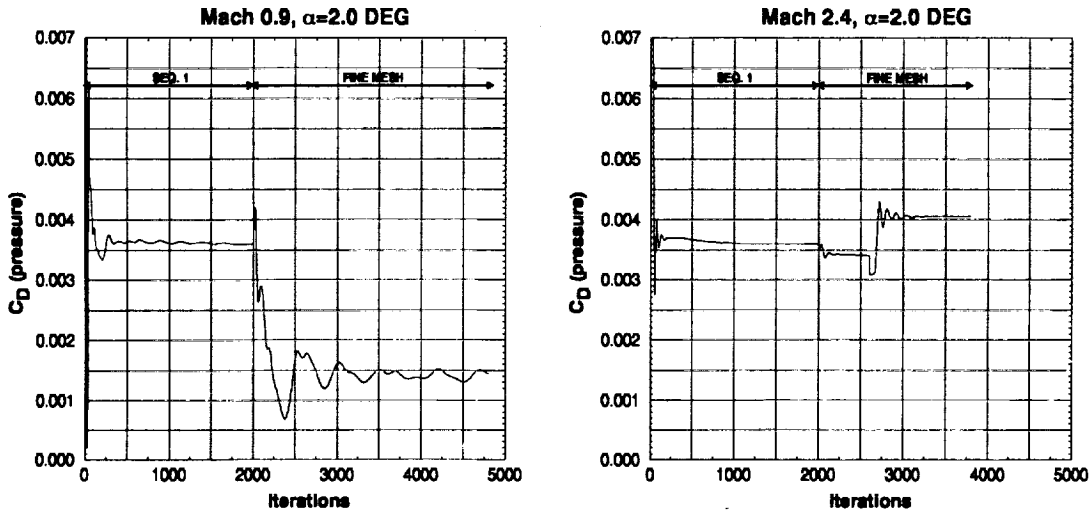

NORTHROP GRUMMAN

The drag convergence histories for the Mach 0.9 and 2.4 cases at 2 degrees angle of attack are shown. In GCNS the pressure drag coefficient was calculated at each iteration, but as a means of reducing processing time, the viscous drag convergence history is not generated by GCNS.. The overlapping region of the wing and body grids was counted twice in GCNS. This method is permissible because only the convergence trend is of interest. Each case was run 2000 iterations on the sequenced grid prior to iterations on the fine mesh.

The pressure drag converged at approximately 36 counts (0.0036) for the Mach 0.9 sequenced grid. Fine mesh iterations began after 2,000 sequenced grid iterations. After 1,500 iterations on the fine mesh (cumulative iteration number 3,500), the pressure drag decreased to approximately 14 counts (0.0014) and oscillated in a 2 count bandwidth. An additional 1,200 fine mesh iterations failed to further damp out this trend. The oscillations in pressure drag are due to the transonic effects in the flowfield.

For the Mach 2.4 case, the sequenced grid converged quickly to 36 counts (0.0036). As in the Mach 0.9 case, the fine mesh iterations began after 2,000 sequenced grid iterations . After 1300 fine mesh iterations (cumulative iteration number 3,300), the pressure drag increased and converged at 41 counts (0.0041) with less than a tenth of a count (0.00001) of variation.

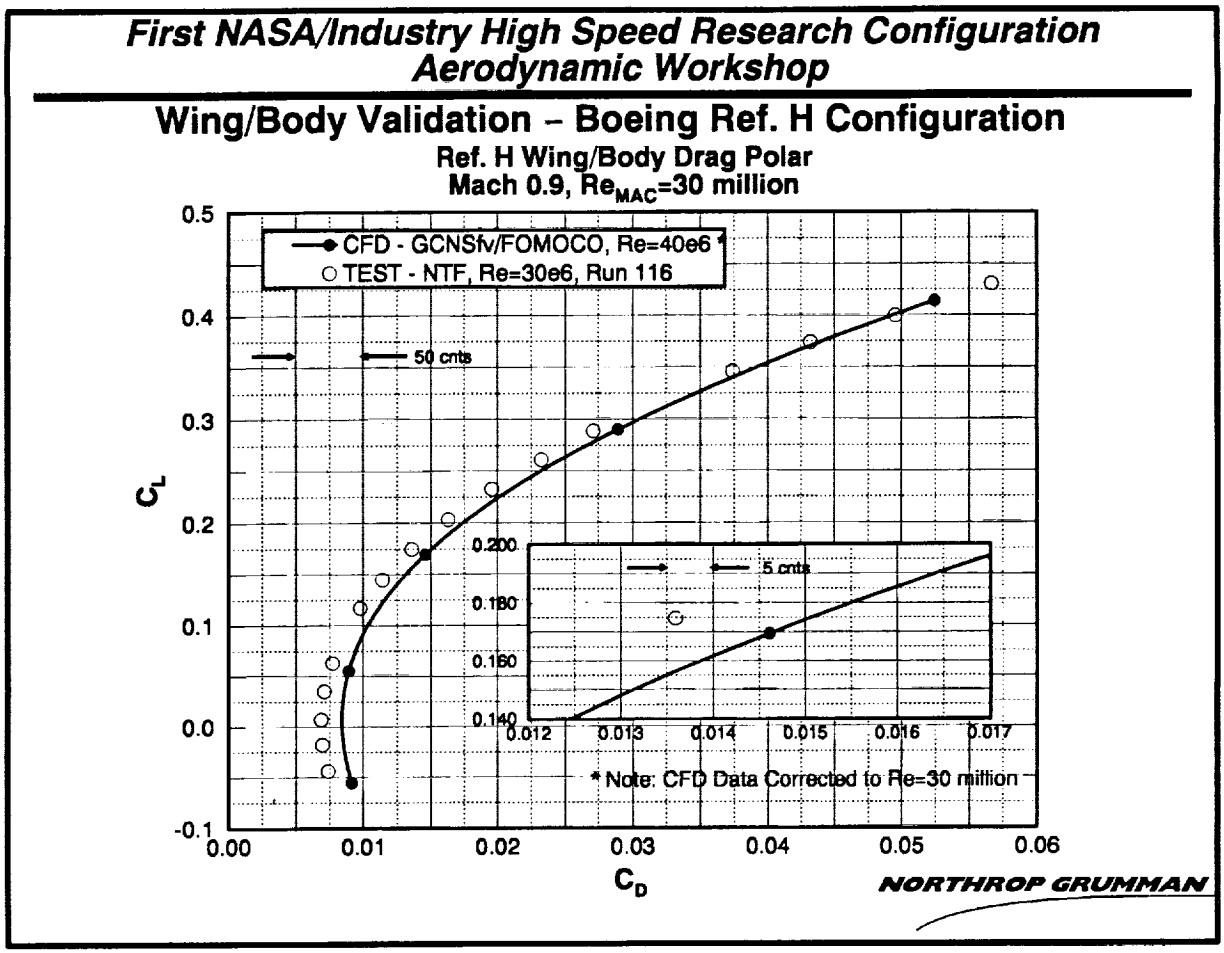

A drag polar for the Mach 0.9 case is shown comparing the CFD analysis to the NTF wind tunnel data. The inset highlights the area around $\alpha=4^{o}$ and shows the CFD data , after correcting to $Re=30x10^{6}$, is about 15 counts high.

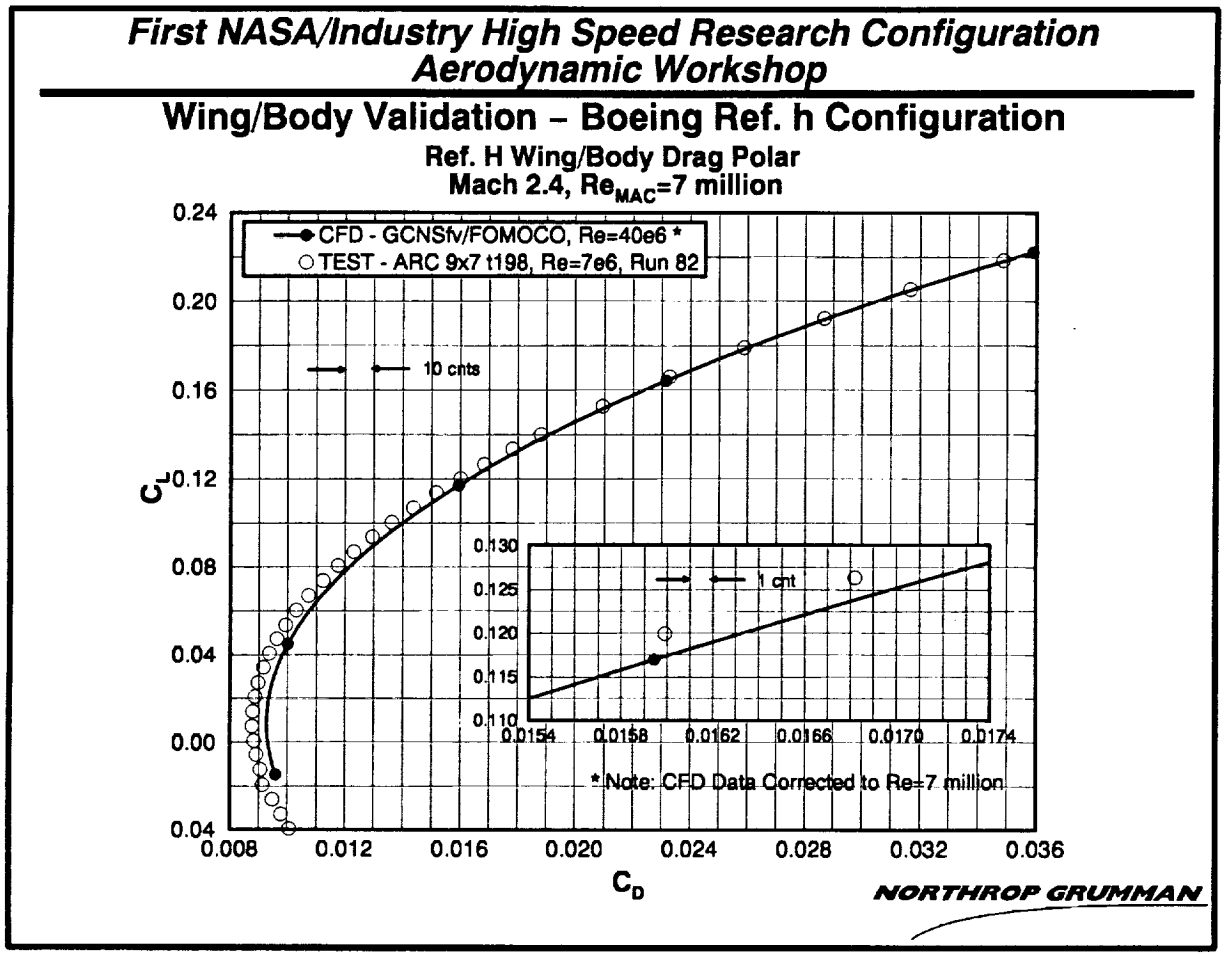

A drag polar for the Mach 2.4 case is shown comparing the CFD analysis to the ARC 9x7 wind tunnel data. The inset highlights the area around the cruise lift point and shows the CFD data , after correcting to Re=7x10^6, is about 3 counts high. This data compared much better than the M=0.9 case.

Isolated Nacelles

- **Model Isolated Nacelle with Transonic and Supersonic Nozzle Settings**
- **Nacelles Run at Zero Angle of Attack with Inlet Face Aligned to the Freestream Flow**
- **Orientation Allowed Half Model to be Generated**
- **Drag Integrations Included Only the External Surfaces**

NORTHROP GRUMMAN

Isolated nacelles were run at M=0.9, 1.1, and 2.4 for the supersonic nozzle setting and at M=0.9 and 1.1 for the transonic nozzle setting. The nacelle geometry was oriented with the inlet face normal to the freestream flow and run at zero angle of attack. Half models of the nacelle were generated using similar grid spacings and topologies as the installed nacelles. The grids for the installed nacelles could not be used directly because they included the integrated diverter. Only the external surfaces were considered in the force integrations. Inlet and nozzle (including the parts of the side walls scrubbed by the nozzle flow) surfaces were not included.

Isolated 2D Nozzle Nacelle – Computational Grid

Supersonic Nozzle

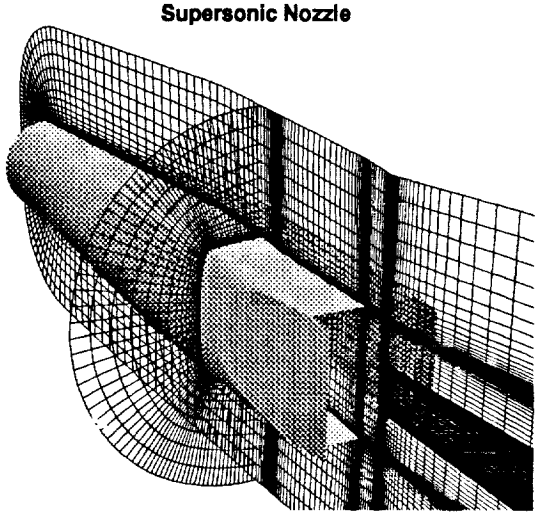

4 Blocks, 1.25 Million Grid points

Transonic Nozzle

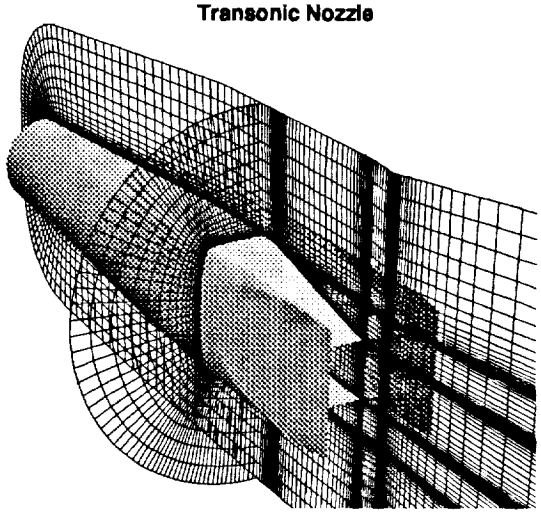

6 Blocks, 1.5 Million Grid points

NORTHROP GRUMMAN

Grids for the isolated nacelles are shown. The supersonic nozzle case used four blocks and 1.25 million grid points and the transonic nozzle case used six blocks and 1.5 million grid points. Both geometries were run half symmetric. Again, to provide grid consistency between cases, the transonic nozzle case used the same nacelle grid as the supersonic nozzle with the addition of two "wedge" blocks to model the deflected nozzle flaps.

First NASA/Industry High Speed Research Configuration Aerodynamic Workshop

Isolated 2D Nozzle Nacelle,Supersonic Configuration

Mach=0.9, NTR=3.264, NPR=5.0

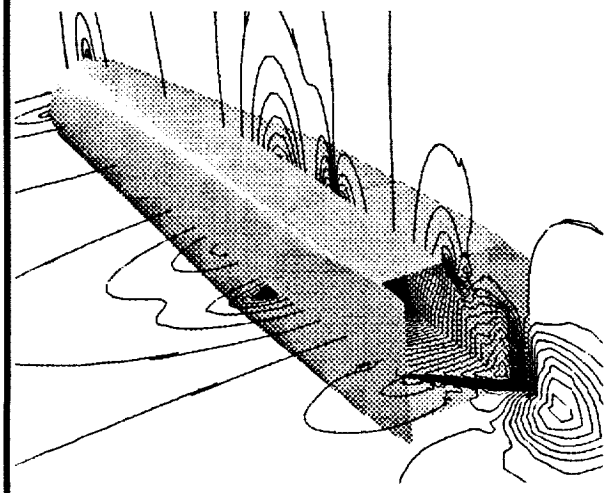

Mach=1.1, NTR=3.056, NPR=5.0

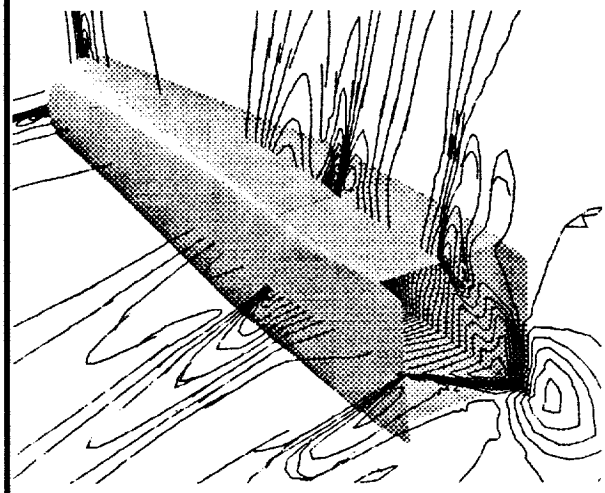

Contours of Cp on the symmetry and half planes

NORTHROP GRUMMAN

Pressure contours on the symmetry and horizontal mid-planes are shown for the isolated nacelle with the supersonic nozzle setting at Mach numbers of 0.9 and 1.1. Effects of the nozzle flap hinge line and the side wall tapering can be seen in the contours but the flow stays attached for both cases.

First NASA/Industry High Speed Research Configuration Aerodynamic Workshop

Isolated 2D Nozzle Nacelle,Transonic Configuration

Mach=0.9, NTR=3.264, NPR=5.0

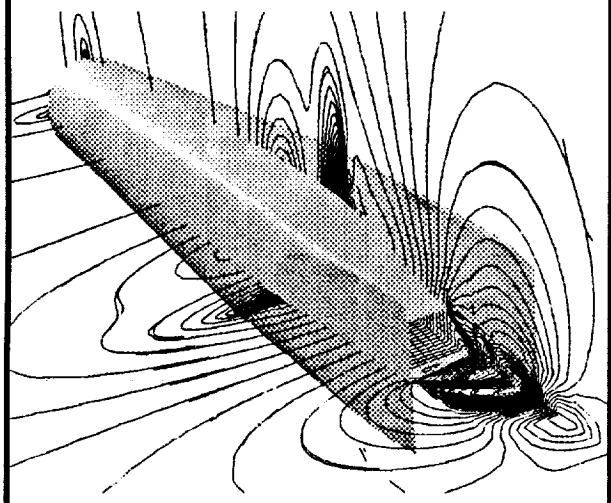

Mach=1.1, NTR=3.056, NPR=5.0

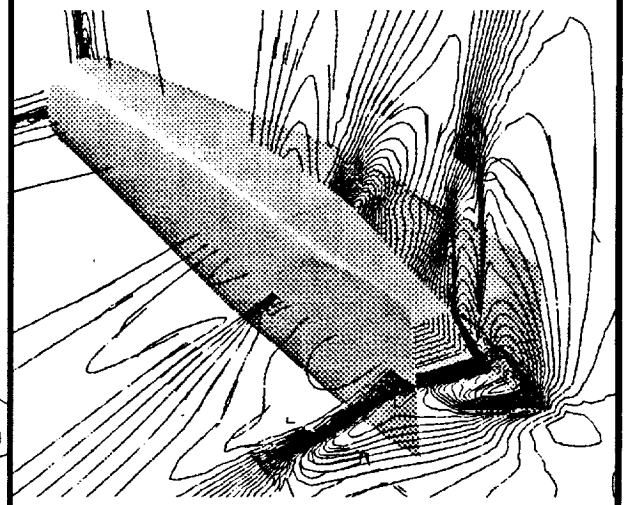

Contours of Cp on the symmetry and half planes

NORTHROP GRUMMAN

Pressure contours on the symmetry and side planes are shown for the isolated nacelle with the transonic nozzle setting at Mach numbers of 0.9 and 1.1. For the M=0.9 case a normal shock develops at the nozzle hinge line, separating the flow over the flap upper surface giving way to a pressure recovery. In the Mach 1.1 case the flow shocks weakly at the hinge line but, stays attached, smoothly recompressing until a normal shock forms at the trailing edge, where the flow is turned by the plume. By staying attached and accelerating over the surface the flow causes a lower pressure region in this case.

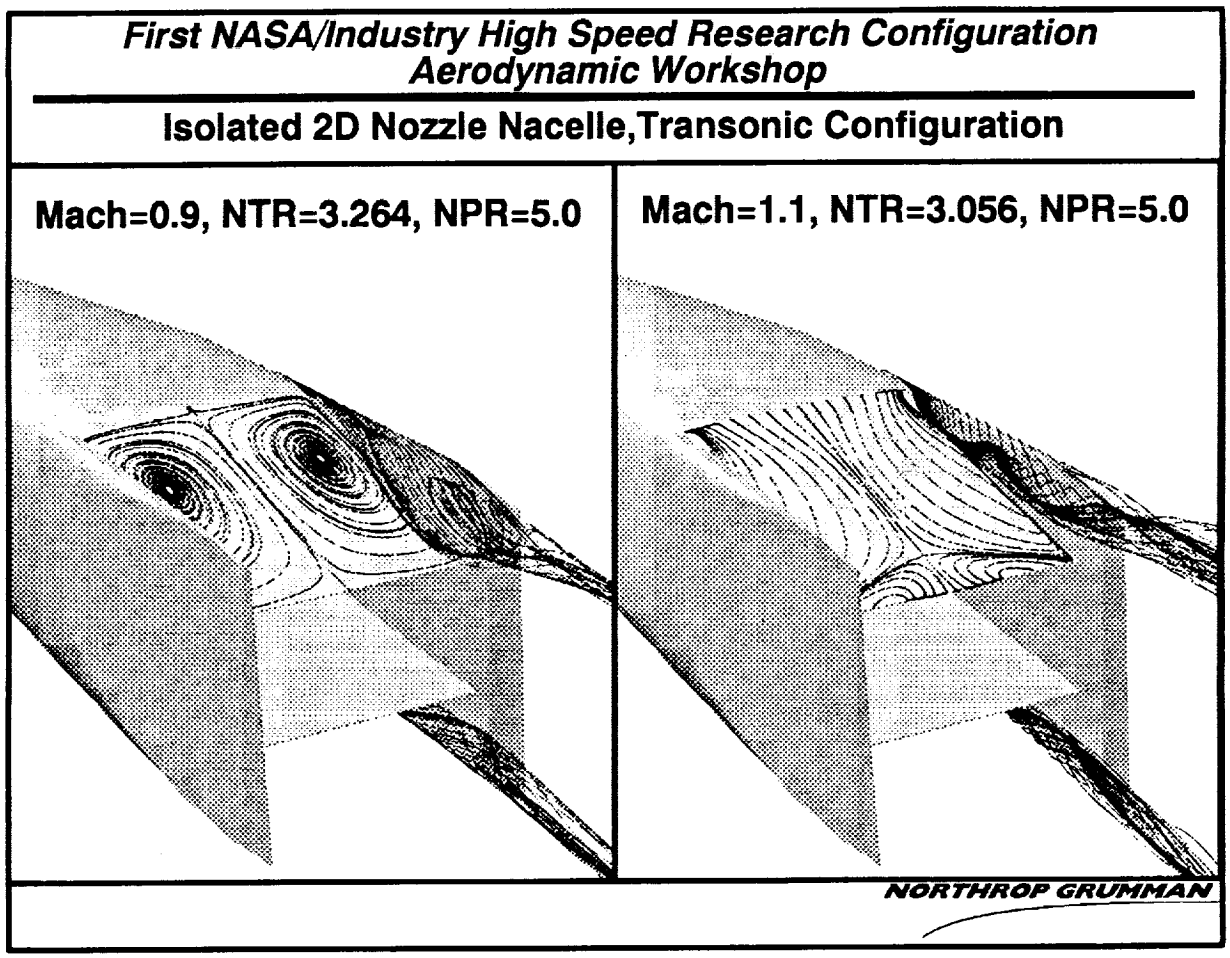

Surface streamlines (simulated oil flow) and streamlines off of the side walls are shown for the isolated nacelle with the transonic nozzle setting for M=0.9 and 1.1. As can be seen from the oil flows for the M=0.9 case the flow is separated over the entire flap upper surface. The surface oil flow for the M=1.1 case shows that the flow stays attached to nearly the nozzle exit.

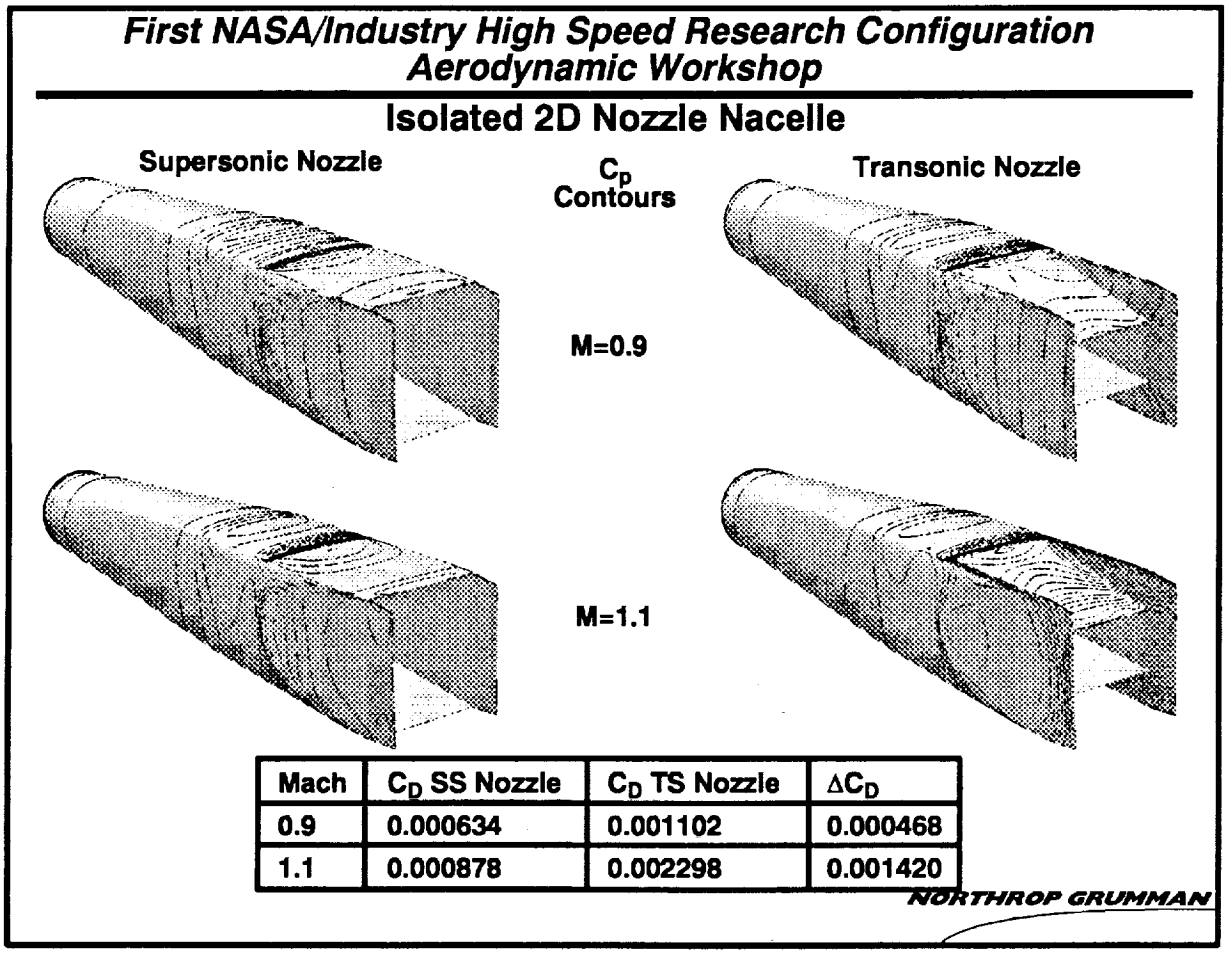

For the thrust/drag bookkeeping, the difference in drag between the isolated nacelles with the supersonic and transonic nozzle settings is considered a thrust term. The geometries for the two configurations with Cp contours on the surface are shown for the Mach 0.9 and 1.1 cases. The table shows the drag values for each configuration and the delta between the supersonic and transonics nozzles which is the "boattail drag".

First NASA/Industry High Speed Research Configuration Aerodynamic Workshop

Wing/Body/Nacelle/Diverter

- **Model Wing/Body/Nacelle/Diverter with Transonic and Supersonic Nozzle Settings**
- **Use the Force Integrations From the Full Configuration, the Wing/Body and the Isolated Nacelles to Determine the Interference Effects**

NORTHROP GRUMMAN

The full configuration (wing/body/nacelle/diverter) was modeled with the supersonic nozzle setting for Mach numbers of 0.9 and 1.1 and α of 4 and 6. The full configuration with the transonic nozzle setting was run at Mach numbers of 0.9 and 1.1 and α of 2, 4 and 6. The force integrations from the full configuration combined, with the wing/body and isolated nacelle forces yield the interference effects.

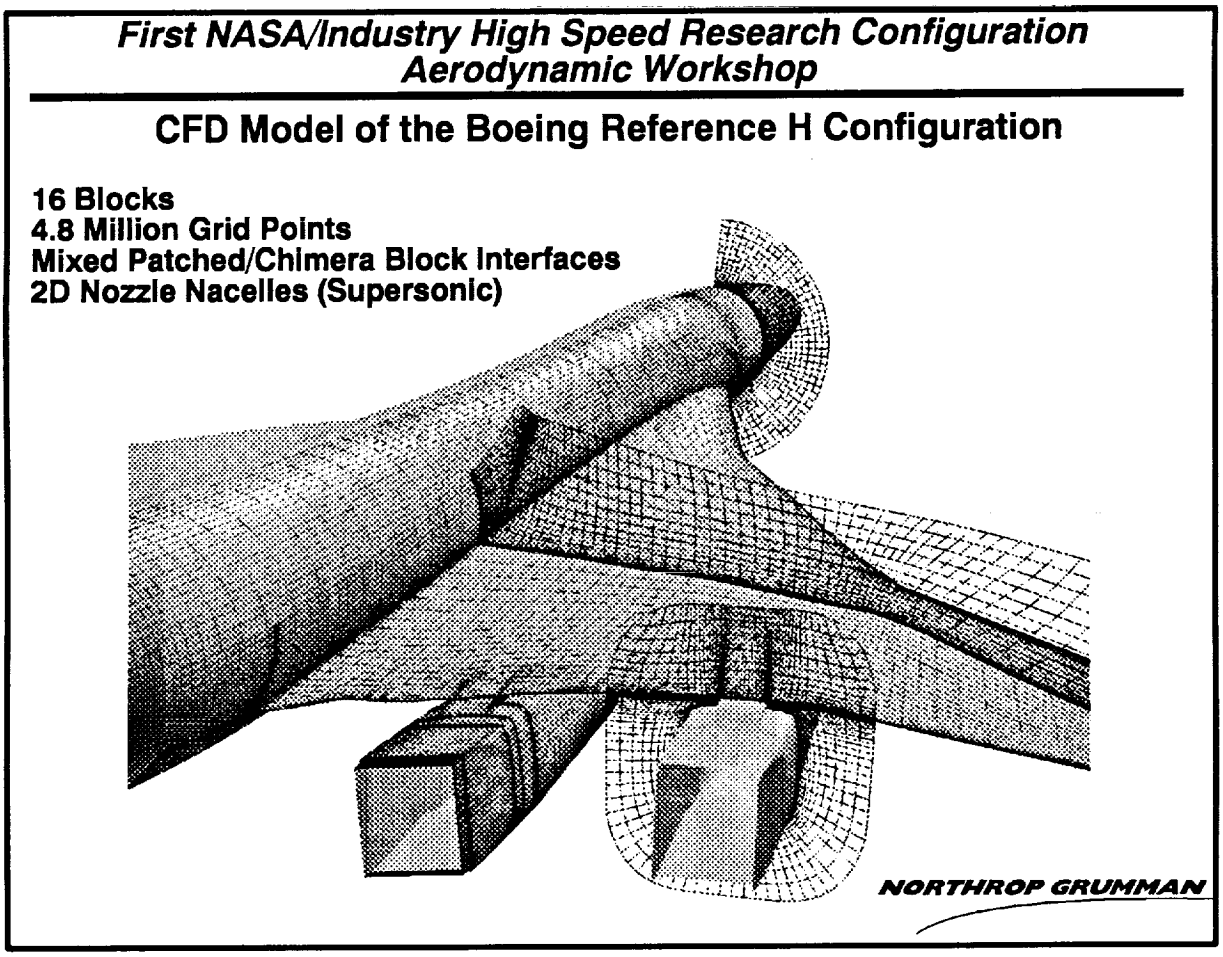

Surface grids and grid topologies for the full configuration (wing/body/nacelles/diverter) with the supersonic nozzle setting are shown. The model consisted of 16 blocks and 4.8 million grid points utilizing both patched and overlapped blocks. The large number of grid points was required to resolve the blunt trailing edges of the nacelle side walls and the nozzle flaps and hinge line. Overlapped (Chimera) blocks were used so that the blocks associated with the nacelle/diverter could easily be removed yielding the wing/body grid. This ensures that the gridding is consistent between the various configurations, eliminating grid changes as a possible influence on drag differences.

CFD Model of the Boeing Reference H Configuration

Ref. H Wing/Body/Nacelle/Diverter Convergence History

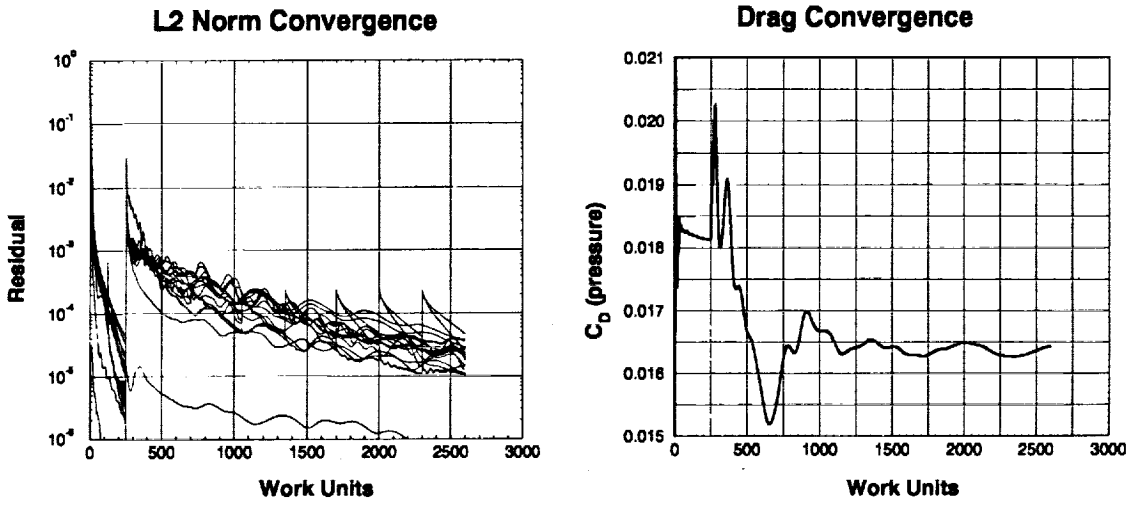

NORTHROP GRUMMAN

Convergence plots for the full configuration (wing/body/nacelle/diverter) with the supersonic nozzle setting are shown. This case was run at M=0.9, α=4° with NPR=5.0 and NTR=3.264, and was used to test out the grid. The residual convergence plots shows the L2 norm of the Q vector as a function of work units (equivalent fine grid iterations) and shows roughly four orders of magnitude drop in residual. The lower sequence level (every other point in each direction) was run for 2000 iterations (250 work units) and the fine mesh for nearly 2500 iterations. The drag convergence plots shows a fluctuation of about 2 counts is still occurring after nearly 2500 iterations on the fine mesh. The range of y+ was 1–3 over the entire vehicle which is adequate for the turbulnece model. The Menter k–ω SST turbulence model was used for this and all the solutions presented. All of the full configuration solutions run to date were run 2000 iterations on the coarse mesh and 3000 iterations on the fine mesh. This took approximately 52 hours of Cray–C90 CPU time and a charged time of 35 hours for utilizing six processors.

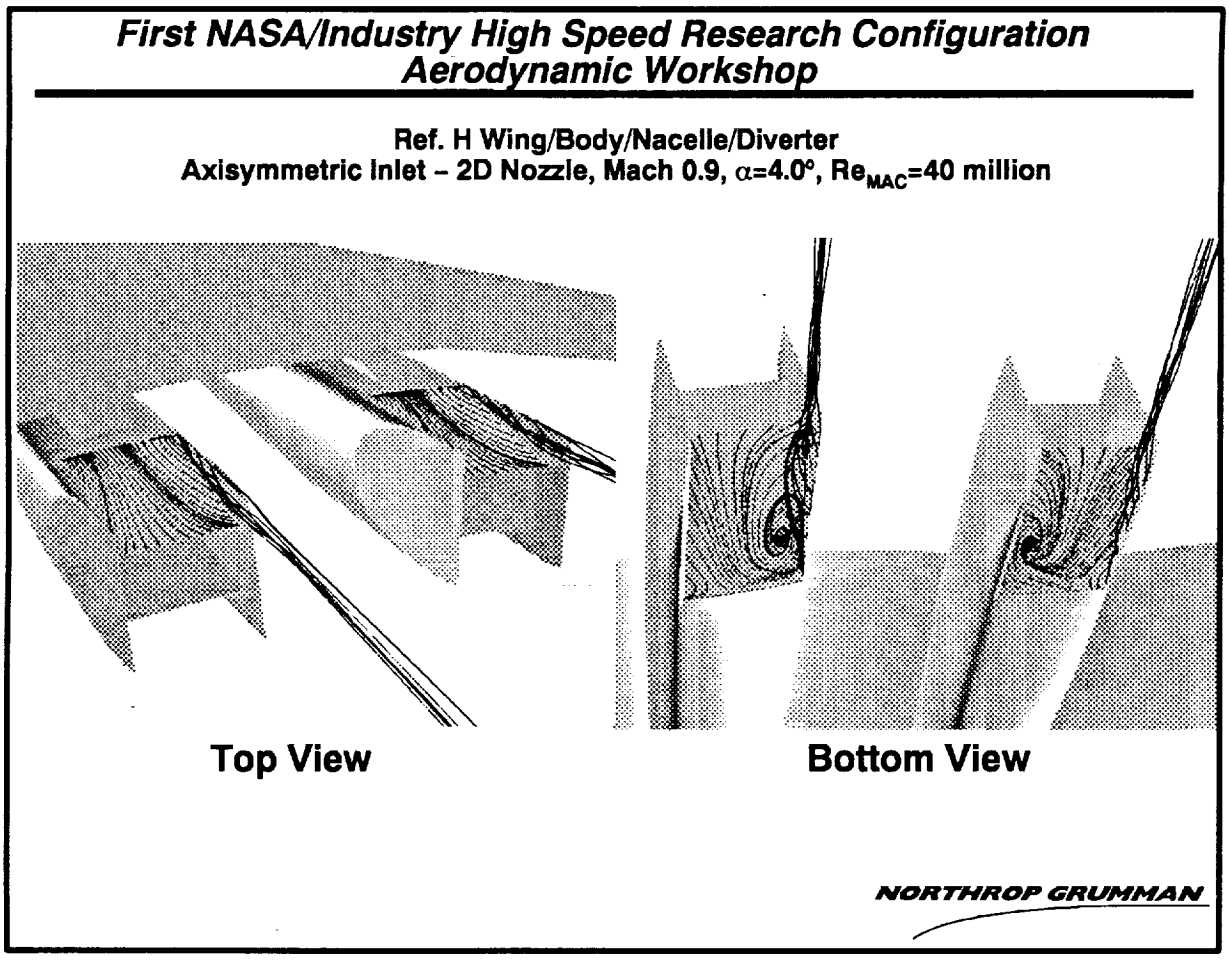

Surface streamlines (oil flows) and streamlines off the outboard side walls are shown for the installed nacelles with the transonic nozzle setting at Mach 0.9. Streamlines on the upper surface show that the flow remains attached over the upper surface due to the flow off of the wing upper surface. The streamlines on the lower surface, however, resemble the isolated nacelle with the nozzle flap fully separated. Nacelle alignment and mutual interference effects give an asymmetric separation on both nacelles.

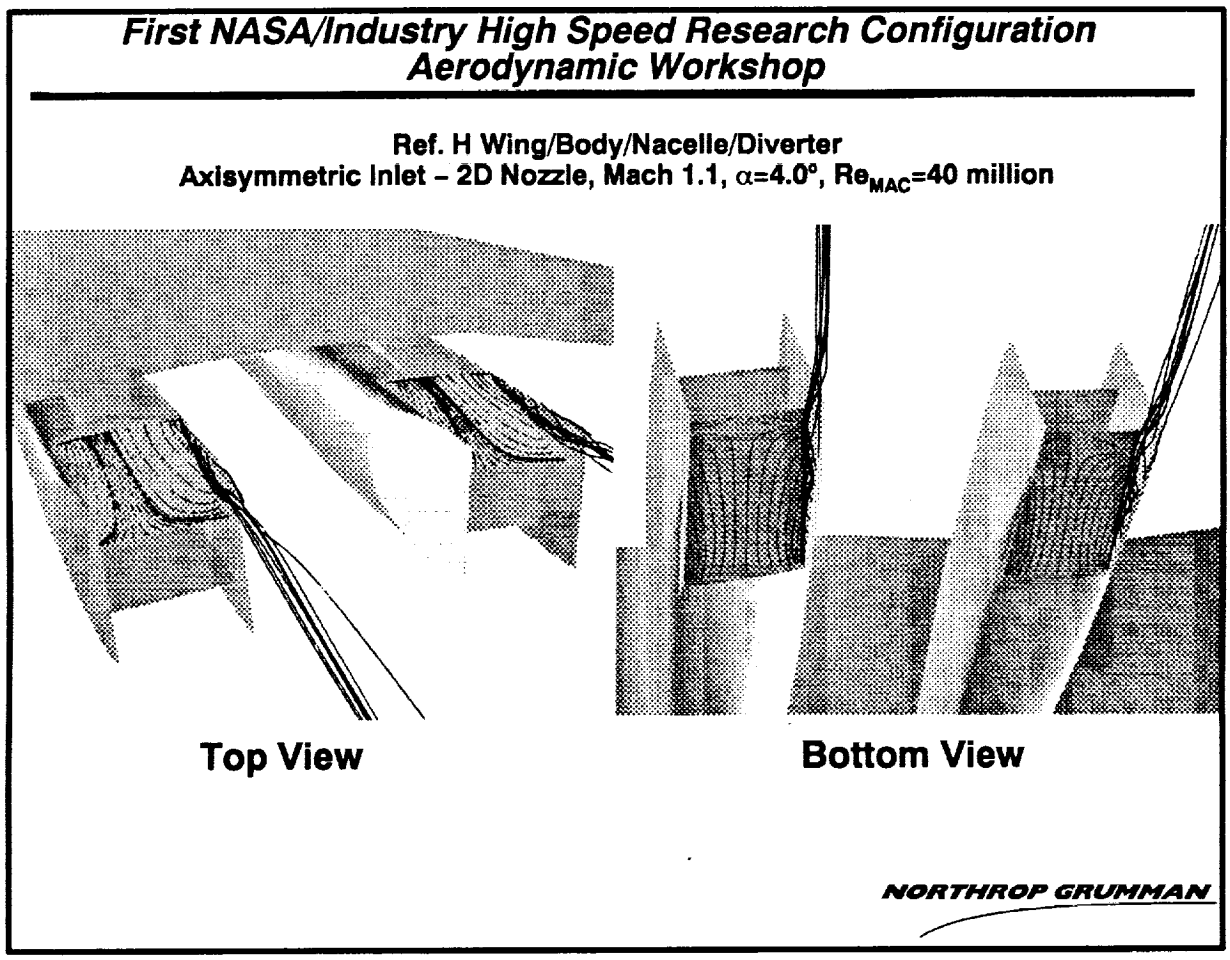

Surface streamlines (oil flows) and streamlines off the outboard side walls are shown for the installed nacelles with the transonic nozzle setting for Mach 1.1. As in the Mach 0.9 case, streamlines on the upper surface show that the flow remains attached over the upper surface due to the flow off of the wing upper surface. The streamlines on the lower surface again resemble the isolated nacelle at this Mach number with the nozzle flap attached until near the nozzle exit.

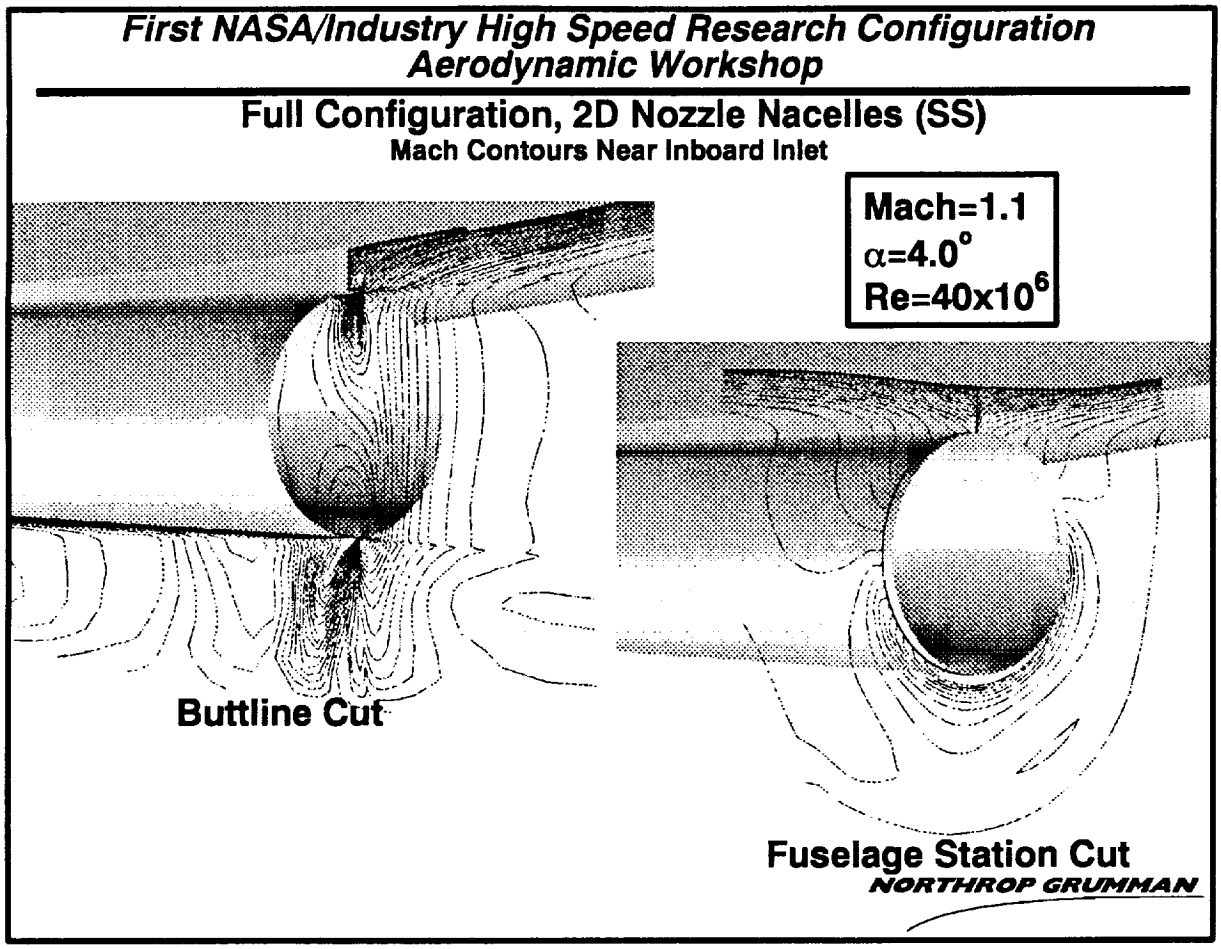

Contours of Mach number near the inlet are shown for the full configuration at Mach 1.1 with the supersonic nozzle setting. While in the isolated nacelle analysis the inlet condition allowed the flow to be swallowed cleanly, the effects of the wing and diverter and the flow alignment of the nacelle itself cause some spillage to occur. Any drag increment due to this spillage is included in the interference drag.

Drag Reduction: Interference Drag

CONSTANT ALPHA

$$CD' = CD_{WBDN} - CD_{isonac,tot,xyz}$$
$$CL' = CL_{WBDN} - CL_{isonac,tot,xyz}$$

WHERE:

$$CD_{isonac,tot,xyz} = [1,0] \bullet \mathbf{CF}_{isonac,tot,xyz}$$
$$CL_{isonac,tot,xyz} = [0,1] \bullet \mathbf{CF}_{isonac,tot,xyz}$$

$$\mathbf{CF}_{isonac,tot,xyz} = [Y]\,[X1]\,\mathbf{CF'}_{isonac_{\alpha=0,x'y'z'}} + [Y][X2]\,\mathbf{CF'}_{isonac_{\alpha=0,x'y'z'}}$$

CF = [CD,CL] aircraft coordinate system

CF' = [CD',CL'] nacelle coordinate system

[X1] , [X2] : transformation matrices to rig inboard and outboard nacelles

$$[Y] = \begin{bmatrix} \sin(\alpha) & \cos(\alpha) \\ \cos(\alpha) & -\sin(\alpha) \end{bmatrix}$$ = transformation matrix to correct for angle of attack to get drag and lift

Internal nacelle forces were not included in force analysis

NORTHROP GRUMMAN

Drag polars (C_D' vs. C_L') were constructed by subtracting the drag and lift contributions of the isolated nacelles from the full configuration. The isolated nacelle forces, **CF'**=[C_D',C_L'] in x',y',z', were transformed from the isolated nacelle coordinate system (x'y'z') to the aircraft coordinate system (xyz). This rigging procedure was done for the inboard and outboard locations. Inboard and outboard transformations are expressed as [X1] and [X2] respectively. The vehicle angle of attack was needed to determine the lift and drag contributions of the isolated nacelles. The use of the [Y] matrix accomplished this transformation.

By subtracting the isolated nacelle forces from the full configuration, we are left with, by definition, wing/body + nacelle interference drag. The forces on the isolated nacelle and the nacelles of the full configuration include the external pressure and viscous forces only. Internal inlet and nozzle forces were not integrated.

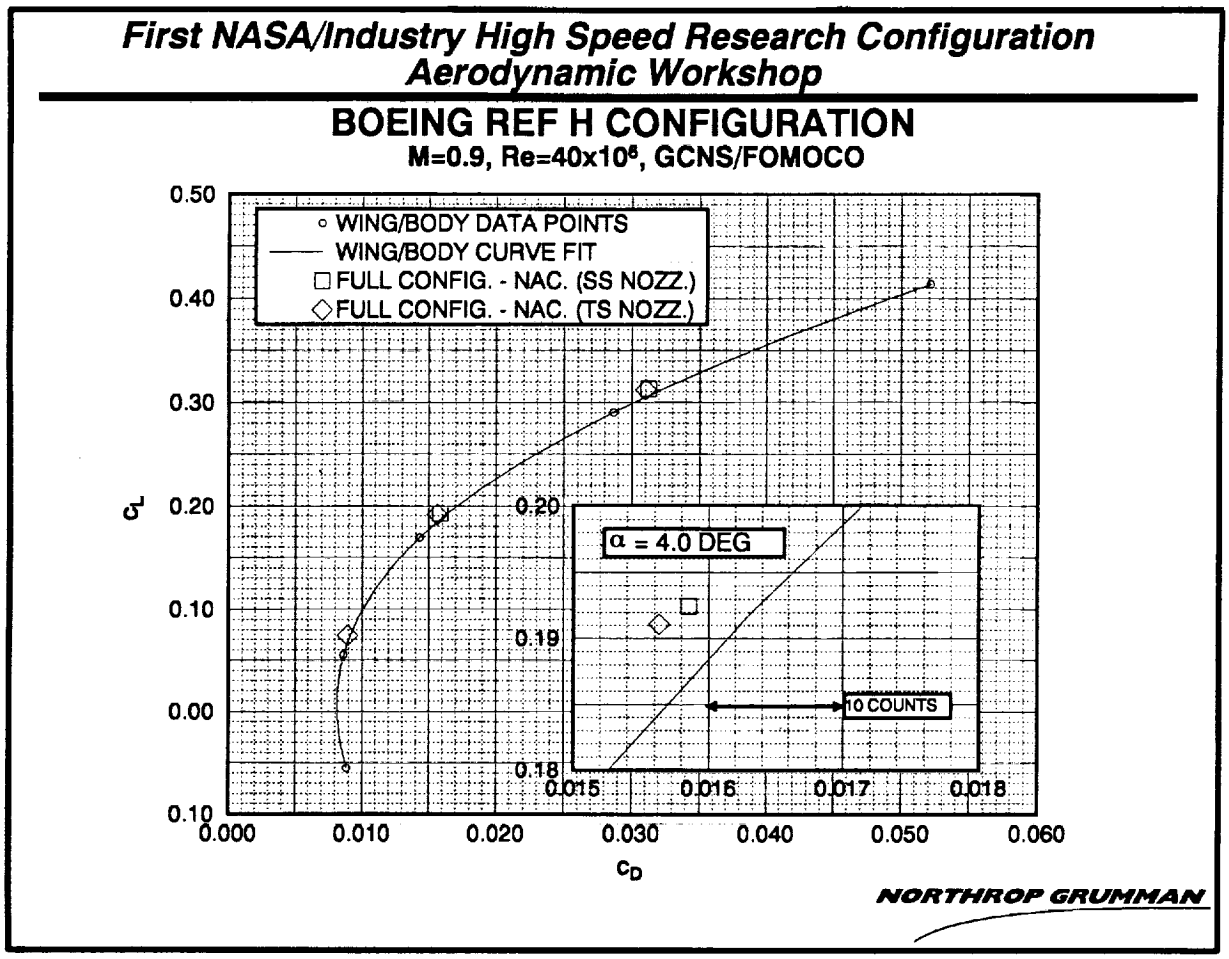

The constructed drag polar (full configuration – isolated nacelle) for M=0.9, Re = $40x10^6$ can be compared to the wing/body case. The difference between them is the nacelle interference drag. These drag polars are shown for the supersonic and transonic nozzle configuration.

For the runs performed, the interference drag is negative in all cases with a constant lift coefficient. The interference drag is determined by comparing the constructed drag polar to the wing/body configuration (see inset) at constant C_L. The drag increment from nacelle interference for the transonic nozzle is −0.00059 (−5.9 counts) at a C_L=0.191. For the supersonic nozzle at a C_L=0.192, the drag increment is −.00049 (−4.9 counts). Both of these points correspond to a full configuration alpha of 4.0 degrees.

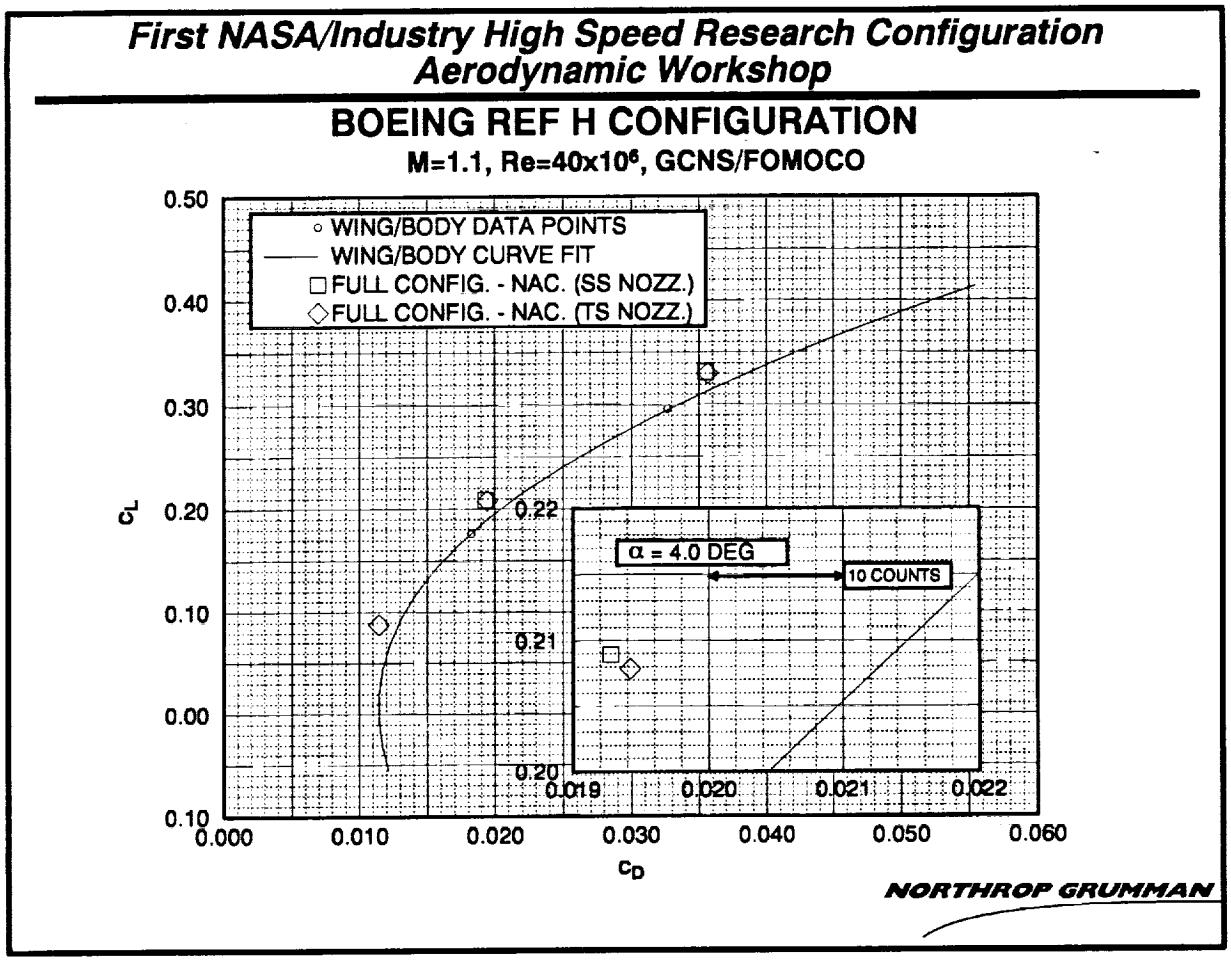

The constructed drag polar (full configuration – isolated nacelle) for M=1.1, Re=40x10^6 can be compared to the wing/body case. The drag polars shown are for the supersonic and transonic nozzle configurations. The wing/body polar was constructed by translating the five five-point curve fit at M=0.9 so that is passed through the two data points run at M=1.1

For the runs performed, the interference drag is again negative in all cases with a constant lift coefficient. The drag increment from nacelle interference for the transonic nozzle is –0.00184 (–18.4 counts) at C_L=0.208. For the supersonic nozzle at C_L=0.209, the drag increment is –.00209 (–20.9 counts). Both of these points correspond to a full configuration alpha of 4.0 degrees.

First NASA/Industry High Speed Research Configuration Aerodynamic Workshop

Conclusions

- **Transonic Nozzle Boattail Drag is Significant for 2D Nozzle Nacelles**
- **Correlation of the Wing/Body Results with Wind Tunnel Data Was Adequate for Force Increments, But Could Be Improved**
- **All Conditions Analyzed Showed Positive Installed Interference Effects**
- **Installed Inlet Spill Effects Due to Local Wing Shape Get Included as Interference Effects**

NORTHROP GRUMMAN

The isolated nacelle analysis showed that the transonic nozzle boattail drag is significant for the 2D nozzle nacelles. Recall the boattail drag is defined as the difference in drag on the isolated nacelle between the supersonic and transonic nozzle settings at a given flow condition. For this study this difference was 4.68 drag counts at M=0.9 and 14.2 drag counts at M=1.1. Comparison of wing/body to full configuration (wing/body/nacelle/diverter) analyses showed positive interference effects for all cases, especially at M=1.1. Correlations between the GCNSfv solutions and the wind tunnel test data for the wing/body configuration leave room for improvement. Aggressive schedule and NAS resource limitations prevented any grid variations to improve correlation with the test data. While the isolated nacelles were run with inlet conditions to give MFR=1.0 and eliminate spill effects from the boattail region this could not be done for the installed nacelles where the flow is influenced by the local wing contouring and nacelle orientation to the flow. The effects of inlet spill get lumped into the interference terms.

First NASA/Industry High Speed Research Configuration Aerodynamic Workshop

Recommendations for Future Work

- **Grid Resolution and Skin Friction Calculations Should be Resolved to Try and Improve the Wing/Body Correlations**
- **Nacelle Placement and Orientation Under the Wing Should Be Optimized for Drag and Inlet Performance**
- **Aft Diverter Height and Aft Diverter-to-Wing Integration Should Be Optimized for 2D Nozzle Nacelles**

NORTHROP GRUMMAN

Effects of grid spacing and resolution as well as the force intergrations should be investigated to try and improve the correlations. Flow near the inlets for the installed nacelles clearly show that the orientation and placement of the nacelles under the wing should be optimized to try and improve drag and inlet performance. Additional analysis should be done to determine the best aft diverter height and aft diverter-to-wing integration to minimize installed boattail drag.